Torque Ripple Minimization in PM Synchronous Motors Using Iterative Learning Control

Weizhe Qian, Sanjib K. Panda, *Senior Member, IEEE*, and Jian-Xin Xu, *Senior Member, IEEE*

***Abstract*—Parasitic torque pulsations exist in permanent magnet synchronous motors (PMSMs) due to nonsinusoidal flux density distribution around the air-gap, errors in current measurements, and variable magnetic reluctance of the air-gap due to stator slots. These torque pulsations vary periodically with rotor position and are reflected as speed ripple, which degrades the PMSM drive performance, particularly at low speeds. Because of the periodic nature of torque ripple, iterative learning control (ILC) is intuitively an excellent choice for torque ripple minimization. In this paper, first we propose an ILC scheme implemented in time domain to reduce periodic torque pulsations. A forgetting factor is introduced in this scheme to increase the robustness of the algorithm against disturbance. However, this limits the extent to which torque pulsations can be suppressed. In order to eliminate this limitation, a modified ILC scheme implemented in frequency domain by means of Fourier series expansion is presented. Experimental evaluations of both proposed schemes are carried out on a DSP-controlled PMSM drive platform. Test results obtained demonstrate the effectiveness of the proposed control schemes in reducing torque ripple by a factor of approximately three under various operating conditions.**

***Index Terms*—Frequency domain design, ILC, parasitic torque pulsations, PMSM, torque ripple minimization.**

I. Introduction

PERMANENT magnet synchronous motors (PMSMs) are widely used in robotics, machine tools and other high-performance industrial servo applications. However, the main disadvantage of PMSMs is the parasitic torque pulsations [1]. Presence of these torque pulsations results in instantaneous torque that pulsates periodically with rotor position. These pulsations are reflected as periodic oscillations in the motor speed, especially at low speed operations. These speed oscillations severely limit the performance of the servo especially in high-precision tracking applications. Moreover, the oscillations produce undesirable mechanical vibration leading to acoustic noise.

There are various sources of torque pulsations in a PMSM such as the cogging, flux harmonics, errors in current measurements and phase unbalancing. In view of the increasing popularity of PMSMs in industrial servo applications, the suppression of pulsating torque has received much attention in recent years. Broadly speaking, these techniques can be divided into two groups: one focusing on the improvement of motor design and the other emphasizing on using active control of stator current excitations [1]. From the motor design viewpoint, skewing the stator lamination stacks or rotor magnets, arranging proper winding distribution and other motor design features reduce cogging torque to a certain degree but do not completely eliminate it [2]. Moreover, special machine design processes additionally increase the complexity in the production process, which result in higher machine cost.

The second approach, which is of our interest, concentrates on using an additional control effort to compensate these periodic torque pulsations. One of the earliest method proposed in [3], [4] is to use pre-programmed stator current excitations to cancel torque harmonic components. However, in such method, sufficiently accurate information of the PMSM parameters, in particular the characteristics of torque ripple are required, and a small error or variations in parameters can lead to an even higher torque ripple due to the open-loop feed-forward control. In view of the inherent limitations of the open-loop feed-forward control scheme, alternative approaches applying closed-loop control algorithms with online estimation techniques (e.g., a self-commissioning scheme [5] and an adaptive control algorithm [6]) to achieve torque pulsation minimization have been proposed. These real-time control schemes are implemented either in speed or in current (torque) loops. In torque control schemes, one popular way is to regulate torque by using online estimated torque based on electrical subsystem variables only. Various algorithms have been proposed for instantaneous torque estimation [7]–[10]. On the other hand, this approach can be used only for those torque ripple components that are observable from electrical subsystem—ripple due to mechanical part (e.g., cogging torque and load oscillations) cannot be observed or controlled. An alternative technique is to use a torque transducer with high bandwidth output to measure the instantaneous torque signal, which can then be applied as the feedback information. This, however, increases the cost of drive system. While all of the techniques described above seek to attenuate torque pulsations by adjusting the stator current excitations, an alternative approach relies on a closed-loop speed regulator to accomplish the same objective indirectly, i.e., the attenuation of torque ripple [6], [8]. All possible sources of torque ripple are observable from rotor speed, and hence this method has potential for complete torque ripple minimization. However, the quality of speed feedback and slow dynamics of the outer speed loop limit the dynamic performance of the algorithm.

In this paper, first we propose an iterative learning control (ILC) scheme implemented in time domain with the objective of minimizing periodic torque ripple. A forgetting factor is introduced in this scheme to increase the robustness of the algorithm against noise, initialization error and fluctuation of system

Manuscript received March 10, 2003; revised June 6, 2003. Recommended by Associate Editor A. Emadi.

The authors are with the Department of Electrical and Computer Engineering, National University of Singapore, Singapore, 117576 (e-mail: eleskp@nus.edu.sg).

Digital Object Identifier 10.1109/TPEL.2003.820537

dynamics. However, this limits the extent to which torque pulsations can be suppressed. To eliminate this limitation of time-domain learning scheme, a modified ILC scheme implemented in frequency domain by means of Fourier series expansion is presented. The proposed ILC controller is implemented in the torque control loop. The performances of both the ILC control schemes have been evaluated through extensive experimental investigations. Test results obtained demonstrate improvements in the steady-state torque response and therefore validate the effectiveness of both proposed ILC schemes in suppressing torque ripple.

The remainder of this paper is organized as follows. In Section II, the mathematical model of the PMSM is given. Section III briefly describes the sources of torque pulsations in PMSM drives. In Section IV, the proposed ILC schemes implemented in time domain as well as in frequency domain are explained. Section VI presents the experimental results, which are obtained from the DSP-controlled PMSM drive system as described in Section V. Finally, concluding remarks are made in Section VII.

II. Dynamic Model of a PMSM

With assumptions that the PMSM is unsaturated and eddy currents and hysteresis losses are negligible [11], the stator d, q-axes voltage equations of the PMSM in the synchronous rotating reference frame are given by

$$\frac{di_{ds}}{dt} = -\frac{R}{L_d} i_{ds} + \frac{L_q}{L_d}\omega_e i_{qs} + \frac{1}{L_d} v_{ds} \tag{1}$$

$$\frac{di_{qs}}{dt} = -\frac{R}{L_q} i_{qs} - \frac{L_d}{L_q}\omega_e i_{ds} - \frac{\omega_e}{L_q}\psi_{dm} + \frac{1}{L_q} v_{qs} \tag{2}$$

where i_{ds} and i_{qs} are the d, q-axes stator currents, v_{ds} and v_{qs} are the d, q-axes voltages, L_d and L_q are the d, q-axes inductances, while R and ω_e are the stator resistance and electrical angular velocity, respectively. The flux linkage ψ_{dm} is due to rotor magnets linking the stator. It has been further assumed that as the surface mounted PMSM is nonsalient, L_d and L_q are equal and are taken as L.

Using the method of field-oriented control of the PMSM, the d-axis current i_{ds} is controlled to be zero to maximize the output torque [12]. The motor torque is given by

$$T_m = \frac{3}{2}\frac{P}{2}\psi_{dm} i_{qs} = k_t i_{qs} \tag{3}$$

in which $k_t (=(3/2)(P/2)\psi_{dm})$ is the torque constant and P is the number of poles in the motor.

The equation of the motor dynamics is

$$\frac{d\omega_m}{dt} = -\frac{B}{J}\omega_m + \frac{k_t}{J} i_{qs} - \frac{T_l}{J} \tag{4}$$

where ω_m is the motor speed, T_l is the load torque, B is the frictional coefficient and J is the total inertia (including motor and load).

III. Analysis of Torque Pulsations

A. Cogging Torque

Cogging torque is produced by the magnetic attraction between the rotor mounted permanent magnets and the stator. It is the circumferential component of attractive force that attempts to maintain the alignment between the stator teeth and the permanent magnets. Cogging torque harmonics appear at frequencies that are multiple of $N_{\text{slot}-\text{pp}} f_s$, where $N_{\text{slot}-\text{pp}}$ is the number of slots per pole pair and f_s is the electrical frequency of the rotor. Analytical modeling of the cogging torque is challenging since its production mechanism involves complex field distributions around stator slots [2]. However, one thing can be assured that cogging torque is a periodic function of rotor position, and this makes it feasible to use the proposed ILC scheme for suppressing the pulsating torque.

B. Flux Harmonics

Another principal source of torque pulsations in PMSMs is the harmonics present in the air-gap flux. In real PMSMs, a perfect sinusoidal flux density distribution around the air gap periphery is difficult to achieve and subject to manufacturing tolerances. This results in a nonperfect sinusoidal flux density distribution which, when interacts with the purely sinusoidal stator currents gives rise to periodic torque ripple [13]. The resultant flux linkage between the permanent magnet and the stator currents contains harmonics of the order of 5, 7, 11, ... in the a-b-c frame (triple harmonics are absent in Y-connected stator windings). In the synchronous rotating reference frame, the corresponding harmonics appear as the sixth, 12th, and other multiples of the sixth harmonics, and can be expressed as

$$\psi_{dm} = \psi_{d0} + \psi_{d6}\cos 6\theta_e + \psi_{d12}\cos 12\theta_e + \cdots \tag{5}$$

where ψ_{d0}, ψ_{d6} and ψ_{d12} are the dc, sixth and 12th harmonic terms of the d-axis flux linkage respectively while θ_e is the electrical angle. Combining (3) and (5), we get

$$\begin{aligned} T_m &= T_0 + T_6\cos 6\theta_e + T_{12}\cos 12\theta_e + \cdots \\ &= T_0 + \Delta T_{m,6} + \Delta T_{m,12} + \cdots \end{aligned} \tag{6}$$

where T_0, T_6 and T_{12} are the dc component, sixth and 12th harmonic torque amplitudes, respectively. Equation (6) indicates that the sixth and 12th torque harmonics produced mainly due to nonsinusoidal flux distribution are periodic in nature.

C. Current Offset Error

The dc offset in stator current measurements also leads to pulsating torque [14]. Stator currents are measured and converted into voltage signals by current sensors and then transformed into digital form by A/D converters. Presence of any unbalanced dc supply voltage in the current sensors and inherent offsets in the analog electronic devices give rise to dc offsets. Letting the dc offset in the measured currents of phases a and b be Δi_{as} and Δi_{bs} respectively, the 'measured' q-axis current i_{qs-AD} will be the actual q-axis current plus the error, hence

$$i_{qs-AD} = i_{qs} + \Delta i_{qs} \tag{7}$$

where

$$\Delta i_{qs} = \frac{2}{\sqrt{3}} \cos(\theta_e + \delta) \sqrt{\Delta i_{as}^2 + \Delta i_{as} \Delta i_{bs} + \Delta i_{bs}^2} \quad (8)$$

and δ is a constant angular displacement dependent on Δi_{as} and Δi_{bs}. As $\theta_e = 2\pi f_s t$, it is shown that Δi_{qs} oscillates at the fundamental electrical frequency. Assuming the measured current exactly follows the reference current, the actual motor current is given by

$$i_{qs} = i_{qs-AD} - \Delta i_{qs} = i_{qs}^* - \Delta i_{qs}. \quad (9)$$

Using (3) and (9), we get

$$T_m = k_t (i_{qs}^* - \Delta i_{qs}) = T_m^* - \Delta T_{m,1}. \quad (10)$$

Substituting (8) into (10), $\Delta T_{m,1}$ can be obtained as

$$\Delta T_{m,1} = k_t \frac{2}{\sqrt{3}} \cos(\theta_e + \delta) \sqrt{\Delta i_{as}^2 + \Delta i_{as} \Delta i_{bs} + \Delta i_{bs}^2}. \quad (11)$$

Equation (11) shows that the offset in current measurement gives rise to a torque oscillation at the fundamental frequency f_s.

D. Current Scaling Error

The output of the current sensor must be scaled to match the input of the A/D converter, and in the digital form, the controller re-scales the value of the A/D output to obtain the actual value of the current. As such, scaling errors of the currents are inevitable in digital controller [14]. Again assuming ideal current tracking, the measured phase currents are

$$i_{as-AD} = i_{as}^* = I \cos \theta_e \quad (12)$$

$$i_{bs-AD} = i_{bs}^* = I \cos\left(\theta_e - \frac{2\pi}{3}\right). \quad (13)$$

Denoting the scaling factors of the phases a and b currents as K_a and K_b, respectively, the phase currents as seen from the controller are

$$i_{as} = I \cos \theta_e / K_a \quad (14)$$

$$i_{bs} = I \cos\left(\theta_e - \frac{2\pi}{3}\right) \Big/ K_b. \quad (15)$$

From similar analysis as in the current offset error, Δi_{qs} can be evaluated as

$$\begin{aligned} \Delta i_{qs} &= i_{qs-AD} - i_{qs} \\ &= \left(\frac{K_a - K_b}{K_a K_b}\right) \frac{I}{\sqrt{3}} \left[\cos\left(2\theta_e + \frac{\pi}{3}\right) + \frac{1}{2}\right]. \end{aligned} \quad (16)$$

From (10) and (16), the torque error is

$$\Delta T_{m,2} = \left(\frac{K_a - K_b}{K_a K_b}\right) \frac{k_t I}{\sqrt{3}} \left[\cos\left(2\theta_e + \frac{\pi}{3}\right) + \frac{1}{2}\right]. \quad (17)$$

Equation (17) shows that the scaling error causes the torque to oscillate at twice the fundamental frequency $2f_s$.

These analyzes indicate that the electromagnetic torque consists of a dc component together with the first, second, sixth, and 12th harmonic components. All these torque pulsations change periodically as the rotor advances during its rotation. For those systems, which operate repetitively over a fixed time or position interval, ILC is the best choice for improving the tracking performance, i.e., to suppress the periodic torque ripple by generating a compensation reference current. Such a scheme is discussed in the following section.

IV. ILC Schemes for PMSM

Iterative learning control is an approach to improving the tracking performance of systems that operate repetitively over a fixed time interval. Much work has been done in recent years on the application of the ILC in servomechanism systems for industrial applications. ILC is actually an error correction algorithm and a memory that stores the previous controller output data and error information. The learning controller calculates the error $e_i(t)$ between the desired output $y_d(t)$ and the actual system output $y_i(t)$, and computes a new control input $u_{i+1}(t)$ which is stored in the memory for use in the next cycle of operation. The new control input is evaluated based on the criterion that the reduction of $e_i(t)$ is guaranteed iteration by iteration [15].

For a qualitative description of the ILC operation, the following dynamic system is considered

$$\begin{aligned} \dot{x}(t) &= ax(t) + bu(t) + \eta(t) \\ y(t) &= cx(t) + \xi(t) \end{aligned} \quad (18)$$

where a and b are piecewise continuous in t for all $t \in [0, T]$, T being the time period of the desired output, and c is differentiable in x and t. $\eta(t)$ and $\xi(t)$ refer to unstructured uncertainties due to state perturbations and random output measurement noises, respectively. For convergence of the ILC system, given Φ as the learning gain, the following criterion must hold [16]:

$$\|I - cb\Phi\| < 1. \quad (19)$$

In the torque ripple minimization scheme, we have adopted a proportional type (P-type) learning controller employing the combined previous cycle feedback (PCF) and current cycle feedback (CCF) scheme. The P-type algorithm is simple to implement, unlike in the differential type (D-type) since differentiation of the torque signal is unnecessary, hence noise build-up in input update caused by the differentiation of torque signal can be avoided. Note that the actual ILC is implemented in terms of rotor position θ_m instead of time t, since the pulsating torque is a periodic function of angular position and the rotor speed is kept only roughly constant. However, for the simplicity to distinguish between two schemes with and without Fourier series expansion, we still call them the time-domain and frequency-domain schemes.

A. ILC Scheme Implemented in Time Domain

In [16], a mathematically rigorous treatment of the robustness and convergence of the P-type learning control algorithm is given. It is found that the introduction of a forgetting factor α

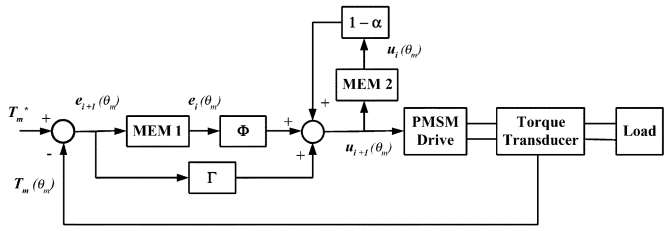

Fig. 1. Block diagram of the ILC scheme implemented in time domain.

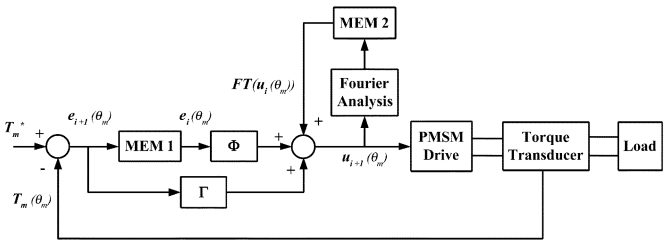

Fig. 2. Block diagram of the ILC scheme implemented in frequency domain.

increases the robustness of the P-type algorithm against noise, initialization error and fluctuation of system dynamics. The proposed ILC scheme in time domain is illustrated in Fig. 1, and the following learning law is used:

$$u_{i+1}(\theta_m) = (1-\alpha)u_i(\theta_m) + \Phi e_i(\theta_m) + \Gamma e_{i+1}(\theta_m) \quad (20)$$

where $u_i(\theta_m)$ is the q-axis reference compensation current from ILC, i.e., Δi_{qs}^*; $e_i(\theta_m)$ is the torque error signal or $T_m^*(\theta_m) - T_m(\theta_m)$; the subscript i is the iteration number; Φ and Γ are the PCF and CCF gains, respectively. From the motor dynamics in (4), and applying (19), the following condition must hold for convergence:

$$\left\| 1 - \frac{k_t}{J}\Phi \right\| < 1. \quad (21)$$

The other requirements of the ILC, which can be satisfied in the reeal-time control of PMSM, are as follows.

- The desired periodic output $y_d(\theta_m)$ is given a priori over the period $2\pi > \theta_m \geq 0$.
- The system must start with the same initial condition in each iteration.
- Invariance of the system dynamics is maintained.
- The output $y_i(\theta_m)$ can be measured within a small specified noise level.

Moreover, with the introduction of forgetting factor, α, the last three conditions can be relaxed to some extent. Unfortunately, this introduction only ensures the tracking errors within a certain bound, and further improvement is limited with the consideration of robustness.

B. ILC Scheme Implemented in Frequency Domain

Under such conditions, we further implemented the learning control in frequency domain by means of Fourier series expansion [17]. Fourier series based learning method enhances the robustness property of iterative learning while maintaining the possibility of reducing tracking errors to zero theoretically. Note that there always exists system noise or other small nonrepeatable factors in the system. Accumulation of those components contained in $u_i(\theta_m)$ may degrade the approximation precision of the controller for each new trial. Fourier series-based learning mechanism, on the other hand, updates coefficients of the learned frequency components over the entire learning period according to (23), which takes an averaging operation on noise and is able to remove the majority of noise and nonrepeatable factors. Consequently, there is no need to introduce the forgetting factor in this scheme. The repeatability of torque ripple implies that only countable integer multiples of the frequency is involved. This ensures the feasibility of constructing component-wise learning in frequency domain. The frequency-domain learning scheme is shown in Fig. 2, and the corresponding control law is given by

$$u_{i+1}(\theta_m) = FT[u_i(\theta_m)] + \Phi e_i(\theta_m) + \Gamma e_{i+1}(\theta_m) \quad (22)$$

with the FT operation defined by (23)–(25), shown at the bottom of the page. Parameter N can be chosen such that Fourier series expansion covers the Nth order of the fundamental frequency, and here it is set to 12.

V. Implementation of Drive System

Fig. 3 shows the overall torque ripple minimization scheme. During the transient state, the ILC is deactivated and the q-axis reference current i_{qs}^* is provided according to the reference torque T_m^*, i.e., $i_{qs}^* = i_{q0}^*$. When steady state is reached, ILC is applied and it provides the additional compensation current Δi_{qs}^* which adds up with i_{q0}^* to produce the final q-axis reference signal i_{qs}^* so as to minimize torque ripple. Conventional PI current controllers that generate the control voltages in accordance with the field-oriented control are used in the inner loop. These current controllers work with a sampling time of 250 μs and the gains are set as: $K_p = 40, K_i = 600$. The learning gains for the proposed ILC scheme are given as: $\Phi = 0.4, \Gamma = 0.02$; forgetting factor $\alpha = 0.05$. Fig. 4 shows the configuration of the experimental setup. A torque transducer is connected along the shaft between the PMSM and the loading system. It has a high bandwidth output (500 Hz), which enables the detection of instantaneous torque. The motor parameters

$$FT[u_i(\theta_m)] = \Psi^T \cdot \frac{2}{2\pi}\int_0^{2\pi} u_i(\theta_m)\Psi_1 d\theta_m \quad (23)$$

$$\Psi = [0.5 \quad \cos\theta_m \quad \cos 2\theta_m \quad \cdots \quad \cos N\theta_m \quad \sin\theta_m \quad \sin 2\theta_m \quad \cdots \quad \sin N\theta_m]^T \quad (24)$$

$$\Psi_1 = [1 \quad \cos\theta_m \quad \cos 2\theta_m \quad \cdots \quad \cos N\theta_m \quad \sin\theta_m \quad \sin 2\theta_m \quad \cdots \quad \sin N\theta_m]^T \quad (25)$$

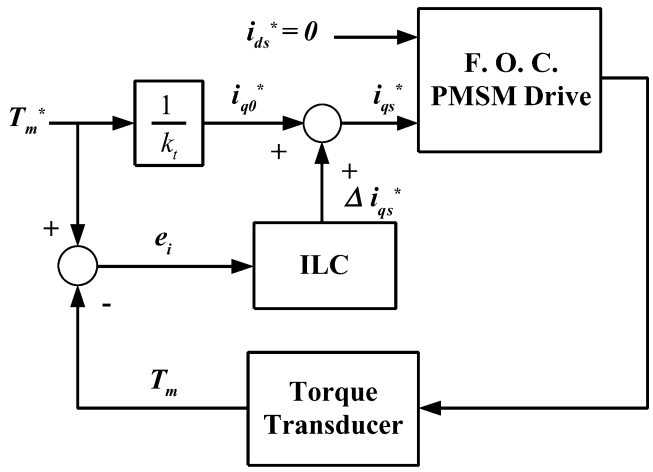

Fig. 3. Block diagram of the torque control loop used in PMSM drive system.

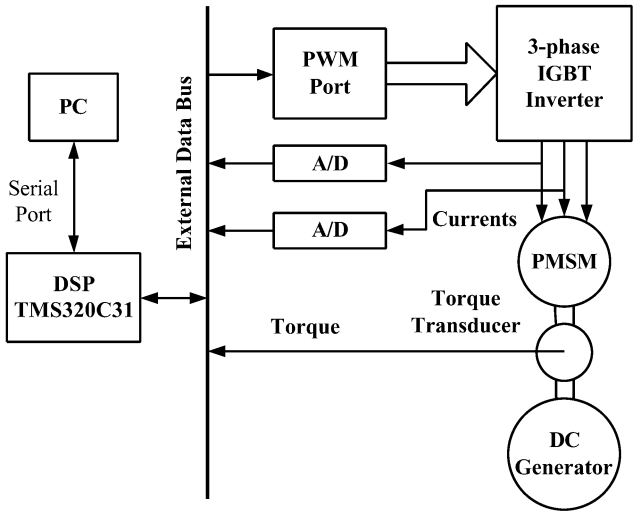

Fig. 4. Configuration of DSP-based experimental setup.

TABLE I
PARAMETERS OF PM SYNCHRONOUS MOTOR

Rated power	1.64 kW
Rated speed	2000 rpm
Stator resistance	2.125 Ω
Stator inductance	11.6 mH
Magnet flux	0.387 Wb
Number of poles	6
Inertia	0.03 kg·m^2

are listed in Table I. The proposed control scheme is realized in the DSP-based drive setup using the floating-point 60 MHz DSP TMS320C31. The control algorithm is implemented using C-program.

The performance evaluation of the proposed ILC control in suppressing torque ripple is presented in the following section.

VI. EXPERIMENTAL RESULTS

To verify the effectiveness of the proposed ILC schemes, experiments are carried out using the DSP-based PMSM drive system as described in Section V. The experiments were conducted under different operating conditions: motor speeds

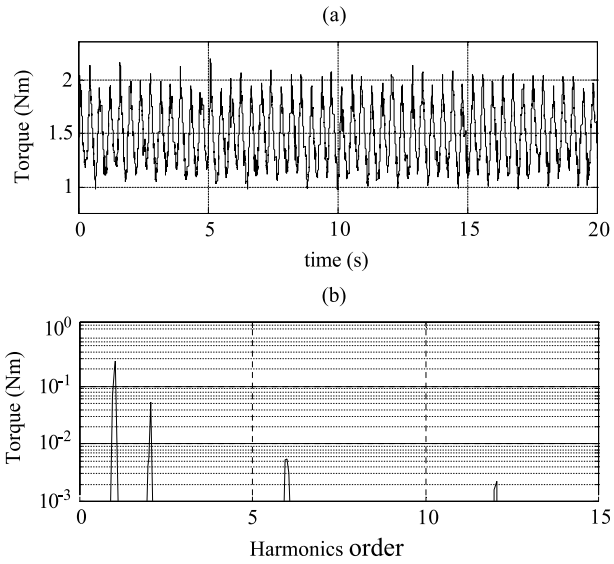

Fig. 5. Torque response without ILC compensation in (a) time domain and (b) frequency spectrum ($\omega_m = 50$ rpm, $T_l = 1.56$ Nm).

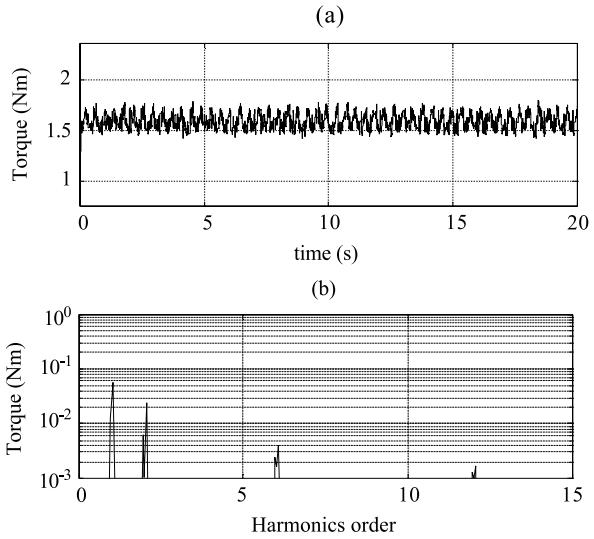

Fig. 6. Torque response with time-domain ILC compensation in (a) time domain and (b) frequency spectrum ($\omega_m = 50$ rpm, $T_l = 1.56$ Nm).

ranging from 0.0125 p.u. (25 rpm) to 0.05 p.u. (100 rpm) and load torques ranging from 0.20 p.u. (1.56 Nm) to 0.795 p.u. (6.20 Nm). The performance criterion used in this work to evaluate the effectiveness of the proposed scheme for torque ripple minimization is the torque ripple factor (TRF). TRF is defined as the ratio of the peak-to-peak torque ripple to the rated torque of the PMSM as shown in (26). The TRF of the drive without ILC compensation is first determined, and subsequently, the compensation reference current generated from ILC is applied and the corresponding TRF is re-evaluated

$$\text{TRF} = \frac{T_{m,pk-pk}}{T_{m,\text{rated}}} \times 100\%. \tag{26}$$

Figs. 5–10 each shows the torque signals in (a) time domain and (b) the corresponding frequency spectrum. For the purpose of clarity, we only pick up the first, second, sixth, and 12th harmonics shown in the frequency spectrum, which are of our in-

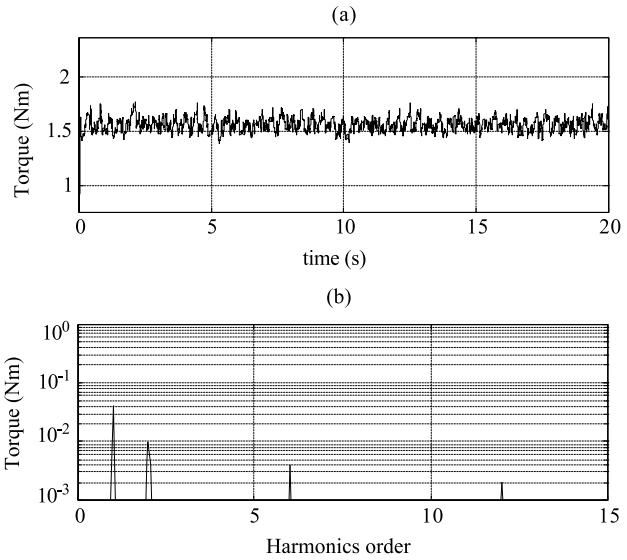

Fig. 7. Torque response with frequency-domain ILC compensation in (a) time domain and (b) frequency spectrum ($\omega_m = 50$ rpm, $T_l = 1.56$ Nm).

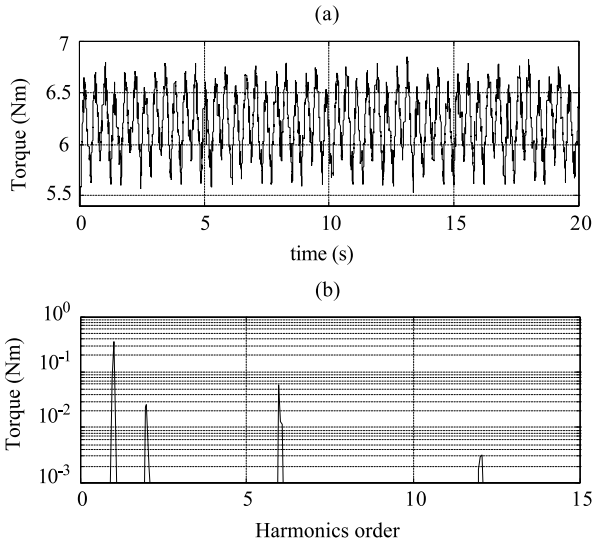

Fig. 8. Torque response without ILC compensation in (a) time domain and (b) frequency spectrum ($\omega_m = 50$ rpm, $T_l = 6.20$ Nm).

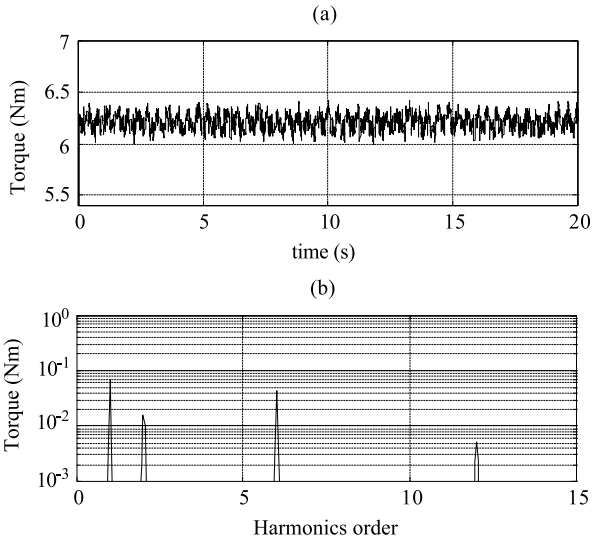

Fig. 9. Torque response with time-domain ILC compensation in (a) time domain, and (b) frequency spectrum ($\omega_m = 50$ rpm, $T_l = 6.20$ Nm).

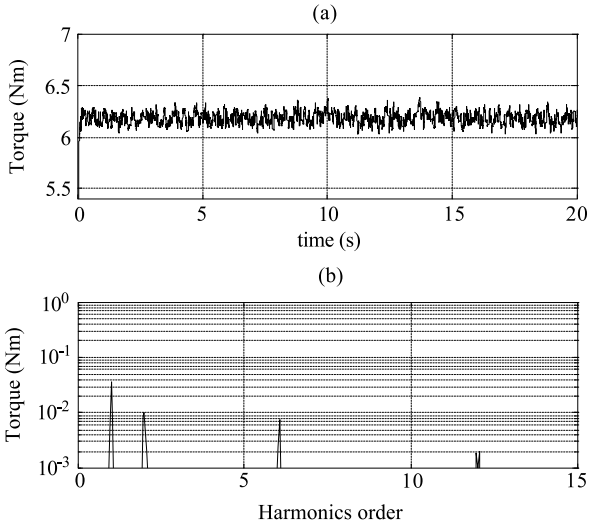

Fig. 10. Torque response with frequency-domain ILC compensation in (a) time domain and (b) frequency spectrum ($\omega_m = 50$ rpm, $T_l = 6.20$ Nm).

terest. Fig. 5 shows the torque response when the motor runs at a speed of 0.025 p.u. (50 rpm), under a light load of 0.20 p.u. (1.56 Nm) without ILC compensation. It can be seen that the torque consists of significant ripple and the corresponding TRF is approximately 14.7%. Figs. 6 and 7 present the torque signals under the same working condition with ILC compensation schemes implemented in time domain and in frequency domain, respectively. With the ILC compensation schemes applied, it is clear that the TRF is reduced from 14.7% (Fig. 5) to 4.3% for the time-domain learning scheme (Fig. 6) and 3.9% for the frequency-domain scheme (Fig. 7).

Figs. 8–10 are arranged in the same sequence, and the operating conditions of these figures are $\omega_m = 0.025$ p.u. (50 rpm), $T_l = 0.795$ p.u. (6.20 Nm). In these cases the corresponding TRF is suppressed from 15.2% to 4.8% and 4.5%, respectively. We can see that pulsating harmonics are reduced after applying the proposed ILC control scheme implemented in time domain, and a further reduction is possible by using the frequency-domain learning method. Comparing the harmonics in Fig. 9 with those in Fig. 10, it can be observed that the first harmonics are reduced to 0.07 Nm and 0.036 Nm by using time-domain and frequency-domain schemes respectively, the second: 0.017 Nm and 0.01 Nm, the sixth: 0.043 Nm and 0.0078 Nm, and the 12th harmonics are suppressed to 0.005 Nm and 0.002 Nm, respectively.

Fig. 11 gives the transient response of motor torque when the ILC compensation scheme is enabled during steady-state operation: $\omega_m = 0.025$ p.u. (50 rpm), $T_l = 0.20$ p.u. (1.56 Nm). It can be observed that after 4 iterations (time period can be calculated as: $T = 60 \times 2/(\omega_m \times P) = 0.4$ s), the torque ripple reaches the maximum reduction. The transient response of motor torque can be seen from Fig. 12 when the reference torque is changed from 3.83 Nm to 3 Nm with the ILC controller applied. In this case, although the motor speed is changed due to the reduction of reference torque, the ILC scheme is not affected

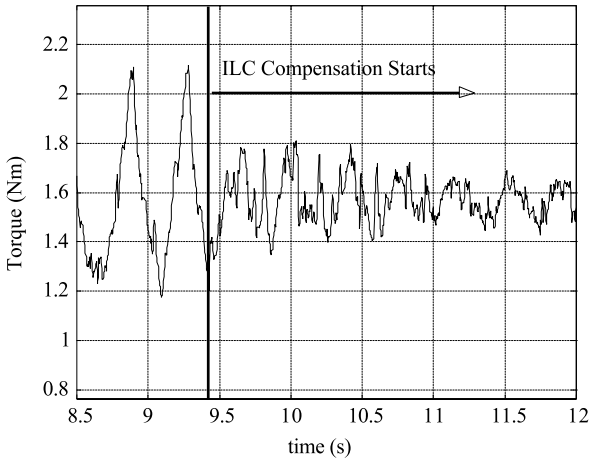

Fig. 11. Transient response of motor torque when the ILC compensation scheme is activated ($\omega_m = 50$ rpm, $T_l = 1.56$ Nm).

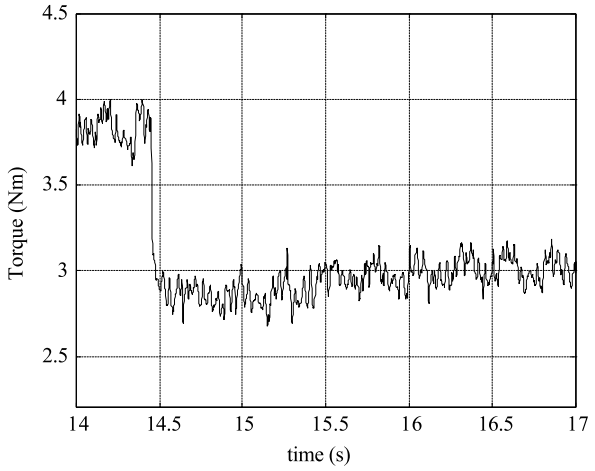

Fig. 12. Transient response of motor torque when the load torque is reduced from 3.83 Nm to 3 Nm with the ILC scheme always on.

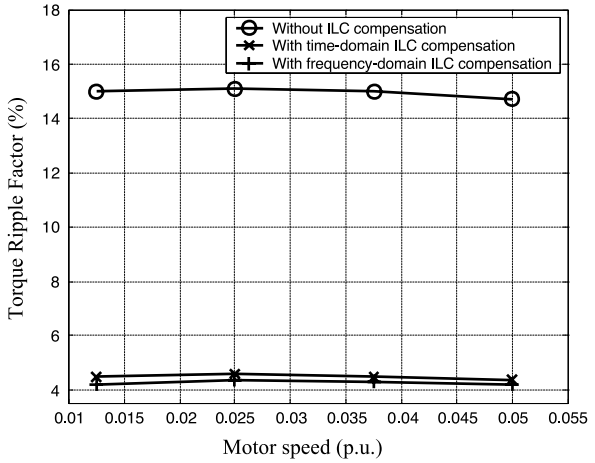

Fig. 13. Detailed TRFs when PMSM operates at different speeds under a heavy load of 5.00 Nm without and with ILC compensation.

because the memory size in the previous controller is fixed, instead of being calculated according to the actual speed, which was reported in [18]. The detailed TRFs for different operating speeds are shown in Fig. 13. It gives the TRFs when PMSM operates at different speeds (0.0125 p.u., 0.025 p.u., 0.0375 p.u. and 0.05 p.u.) under a heavy load of 0.64 p.u. (5.00 Nm) without and with ILC compensation. According to the results, the effectiveness of the proposed ILC schemes is verified in suppressing torque ripple by at least three times under various steady-state operating conditions.

Apparently, the ILC scheme implemented in frequency domain by means of Fourier series expansion is better than that implemented in time domain. This is because the time domain learning cannot eliminate errors completely due to the introduction of forgetting factor [16]. On the other hand, Fourier series expansion keeps the necessary information of the integer harmonics present in control signal, while removing the white noise through the integration of coefficients over the entire learning period. However, ideally it is expected that with frequency-domain learning implementation the torque ripple can be completely eliminated, it cannot be achieved practically and needs further investigations.

VII. Conclusion

Two periodic torque ripple minimization schemes using iterative learning control implemented in time domain and in frequency domain have been presented in this paper. ILC is intuitively an excellent choice for the torque ripple minimization scheme because of the periodic nature of torque ripple. Moreover, being a plug-in module, the scheme is simple to implement, can be added to any existing controller and does not require accurate knowledge of the motor parameters. The performances of both ILC control schemes have been evaluated through experimental investigations. Test results presented demonstrate improvements in the steady-state torque response and therefore validate the effectiveness of both proposed ILC schemes in suppressing torque ripple.

References

[1] T. M. Jahns and W. L. Soong, "Pulsating torque minimization techniques for permanent magnet ac drives—A review," *IEEE Trans. Ind. Electron.*, vol. 43, pp. 321–330, Apr. 1996.

[2] C. Studer, A. Keyhani, T. Sebastian, and S. K. Murthy, "Study of cogging torque in permanent magnet machines," in *Proc. IEEE 32nd Ind. Appl. Soc. (IAS) Annu. Meeting*, vol. 1, New Orleans, LA, Oct. 1997, pp. 42–49.

[3] J. Y. Hung and Z. Ding, "Design of currents to reduce torque ripple in brushless permanent magnet motors," *Proc. Inst. Elect. Eng. B*, vol. 140, no. 4, pp. 260–266, 1993.

[4] D. C. Hanselman, "Minimum torque ripple, maximum efficiency excitation of brushless permanent magnet motors," *IEEE Trans. Ind. Electron.*, vol. 41, pp. 292–300, June 1994.

[5] J. Holtz and L. Springob, "Identification and compensation of torque ripple in high-precision permanent magnet motor drives (Invited paper)," *IEEE Trans. Ind. Electron.*, vol. 43, pp. 309–320, Apr. 1996.

[6] V. Petrovic, R. Ortega, A. M. Stankovic, and G. Tadmor, "Design and implementation of an adaptive controller for torque ripple minimization in PM synchronous motors," *IEEE Trans. Power Electron.*, vol. 15, pp. 871–880, Sept. 2000.

[7] T. S. Low, T. H. Lee, K. J. Tseng, and K. S. Lock, "Servo performance of a BLDC drive with instantaneous torque control," *IEEE Trans. Ind. Applicat.*, vol. 28, pp. 455–462, Apr. 1992.

[8] N. Matsui, T. Makino, and H. Satoh, "Autocompensation of torque ripple of direct drive motor by torque observer," *IEEE Trans. Ind. Applicat.*, vol. 29, pp. 187–194, Feb. 1993.

[9] S. K. Chung, H. S. Kim, C. G. Kim, and M.-J. Youn, "A new instantaneous torque control of PM synchronous motor for high-performance direct-drive applications," *IEEE Trans. Power Electron.*, vol. 13, pp. 388–400, May 1998.

[10] F. Colamartino, C. Marchand, and A. Razek, "Torque ripple minimization in permanent magnet synchronous servodrive," *IEEE Trans. Energy Conv.*, vol. 14, pp. 616–621, Sept. 1999.
[11] P. C. Krause, *Analysis of Electric Machinery*. New York: McGraw-Hill, 1987.
[12] F. Blaschle, "The principle of field orientation as applied to the new TRANSVEKTOR closed-loop control system for rotating-field machines," *Siemens Rev.*, vol. 34, pp. 217–220, May 1972.
[13] B. H. Ng, M. F. Rahman, T. S. Low, and K. W. Lim, "An investigation into the effects of machine parameters on the torque pulsations in a brushless dc drive," in *Proc. IEEE Int. Conf. Elect., Contr. Instrum. (IECON)*, Oct. 24–28, 1988, pp. 749–754.
[14] D. W. Chung and S. K. Sul, "Analysis and compensation of current measurement error in vector-controlled ac motor drives," *IEEE Trans. Ind. Applicat.*, vol. 34, pp. 340–345, Mar./Apr. 1998.
[15] Z. Bien and J.-X. Xu, *Iterative Learning Control—Analysis, Design, Integration and Applications*. Boston, MA: Kluwer, 1998.
[16] S. Arimoto, T. Naniwa, and H. Suzuki, "Robustness of P-type learning control with a forgetting factor for robotic motions," in *Proc. 29th IEEE Conf. Decision Contr.*, vol. 5, Dec. 5–7, 1990, pp. 2640–2645.
[17] J.-X. Xu and W.-J. Cao, "Learning variable structure control approaches for repeatable tracking control tasks," *Automatica*, vol. 37, no. 7, pp. 997–1006, July 2001.
[18] B. H. Lam, S. K. Panda, J.-X. Xu, and K. W. Lim, "Torque ripple minimization in PM synchronous motor using iterative learning control," in *Proc. 25th IEEE Annu. Conf. Ind. Electron. Soc. (IECON'99)*, vol. 3, 1999, pp. 1458–1463.

Weizhe Qian received the B.Eng. degree in electric power engineering from Shanghai Jiao Tong University, China, in 2001 and is currently pursuing the M.S. degree in the Department of Electrical and Computer Engineering, National University of Singapore.

Ms. Qian received the Research Scholarship Award from the National University of Singapore.

Sanjib K. Panda (S'86–M'91–SM'03) received the B.Eng. degree (with first class honors) from REC, Surat, India, in 1983, the M.Tech. degree from IT, BHU, India, in 1987, and the Ph.D. degree from the University of Cambridge, U.K., in 1991, all in electrical engineering.

Since 1992, he has been a Faculty Member in the Department of Electrical and Computer Engineering, National University of Singapore, where he is currently serving as an Associate Professor. He has published over 70 peer-reviewed journal and conference papers. His research interests are control of electric drives, power electronics, power quality, and piezoelectric actuators.

Dr. Panda received the Nehru Cambridge Fellowship jointly awarded by the Nehru Trust for Cambridge University and Cambridge Commonwealth Trust in 1987 and the IEEE Millennium Medal. He is Deputy-Chairman of the IEEE Singapore Section. He also served as the Technical Program Chairman of the PEDS'97 Conference. He is the Conference Organizing Chairman of PEDS'03.

Jian-Xin Xu (M'92–SM'98) received the Ph.D. degree from the University of Tokyo, Tokyo, Japan, in 1989.

He did his Post-Doctoral research at The Ohio State University, Columbus, from 1990 to 1991, and is now an Associate Professor with the National university of Singapore. He has been working in the fields of robust control and intelligent control, in particular variable structure control and constructive learning control. Currently his research focuses on finite interval and infinite interval learning control theory based on function approximation (using contraction mapping, Lyapunov methods, wavelet, etc.), adaptive control of time varying parameters, optimal/sub-optimal sliding mode control, and closed-loop filtering techniques. He has been working for a number of application projects, including micro-nano scale precision servo, electrical drives, freeway traffic, batch reaction process, and robotics, etc. He has published over 90 peer-reviewed journal papers, over 150 papers in prestigious conference proceedings, and co-authored four books with two about variable structure control and two about iterative learning control.